Virus-Mimic mRNA Vaccine for Cancer Treatment

Chaoyang Meng, Zhe Chen, Junhua Mai, Qing Shi, Shaohui Tian, Louis Hinkle, Jun Li, Zhe Zhang, Maricela Ramirez, Licheng Zhang, Yitian Xu, Jilu Zhang, Ping-Ying Pan, Shu-Hsia Chen, Hangwen Li, and Haifa Shen*

An effective therapeutic cancer vaccine should be empowered with the capacity to overcome the immunosuppressive tumor microenvironment. Here, the authors describe a mRNA virus-mimicking vaccine platform that is comprised of a phospholipid bilayer encapsulated with a protein-nucleotide core consisting of antigen-encoding mRNA molecules, unmethylated CpG oligonucleotides and positively charged proteins. In cell culture, VLVP potently stimulated bone marrow-derived dendritic cells (BMDCs) to express inflammatory cytokines that facilitated dendritic cell (DC) maturation and promoted antigen processing and presentation. In tumor-bearing mice, VLVP treatment stimulated proliferation of antigen-specific CD8+T cells in the lymphatic organs and T cell infiltration into the tumor bed, resulting in potent anti-tumor immunity. Cytometry by time of flight (CyTOF) analysis revealed that VLVP treatment stimulated a 5-fold increase in tumor-associated CD8+DCs and a 4-fold increase in tumorinfiltrated CD8+T cells, with concurrent decreases in tumor-associated bone marrow-derived suppressor cells and arginase 1- expressing suppressive DCs. Finally, CpG oligonucleotide is an essential adjuvant for vaccine activity. Inclusion of CpG not only maximized vaccine activity but also prevented PD-1 expression in T cells, serving the dual roles as a potent adjuvant and a checkpoint blockade agent.

1. Introduction

Eversince successful demonstration of protein expression from in vitro-transcribed messenger RNA (IVT mRNA),[1,2] there has been growing interest in applying mRNA for therapeutic interventions.[3] Advances in RNA technology such as codon optimization, nucleotide modification, and large-scale production have allowed speedy clinical application of mRNA-based therapeutic agents.[4,5] The advantage is highlighted by the recent success of vaccines against the SARS-CoV-2 virus, as the first two vaccines approved by the US Food and Drug Administration (FDA) for prevention of COVID-19 are both mRNA-based and the overall development process was completed within 12 months.[6,7] It is anticipated that the enthusiasm will quickly spread to other areas of research and development including therapeutic cancer vaccine,[8] an area that has shown potential in recent clinical trials.[9,10]

In contrast to vaccines for most infectious diseases that rely mainly on antibodies to exert their protective activities, a therapeutic cancer vaccine functions by stimulating Th1-biased activities including proliferation of antigen-specific cytotoxic CD8+ T lymphocytes.[11,12] Since a growing tumor secretes a large quantity of cytokines and chemokines that trigger release of immature myeloid-derived suppressor cells (MDSCs) from the bone marrow, the body is overwhelmed with immunosuppressive cells which produce Th2-biased cytokines, creating a vicious cycle to dampen the body's immune system.[13,14] Thus, an effective therapeutic cancer vaccine should be capable of

C. Meng[+], Z. Chen, J. Mai, Q. Shi, S. Tian, L. Hinkle, J. Li, Z. Zhang, M. Ramirez, H. Shen
Department of Nanomedicine
Houston Methodist Academic Institute
Houston, TX 77030, USA
E-mail: hshen@houstonmethodist.org

The ORCID identification number(s) for the author(s) of this article can be found under https://doi.org/10.1002/adtp.202100144

[+]Present address: Department of Hepatobiliary and Pancreatic Surgery, First Affiliated Hospital, Zhejiang University School of Medicine, Hangzhou 310009, China

C. Meng[+], Z. Chen, S. Tian, J. Li
Xiangya Hospital of Central South University
Changsha, Hunan 410000, China

L. Zhang, Y. Xu, J. Zhang, P.-Y. Pan, S.-H. Chen
Center for Immunotherapy Research
Houston Methodist Academic Institute
Houston, TX 77030, USA

P.-Y. Pan, S.-H. Chen, H. Shen
Weill Cornell Medical College
New York, NY 10065, USA

H. Li
StemiRNA Therapeutics Inc
Shanghai 201206, China

overcoming the immunosuppressive tumor microenvironment and promoting potent Th1-biased immune responses. This is on top of a special requirement for mRNA vaccines to protect mRNA from degradation and to facilitate cell entry of the negatively charged mRNA molecules. Interestingly, liposome-based lipid nanoparticles (LNPs) have been chosen as the delivery vehicle for the above-mentioned FDA-approved mRNA vaccines. LNPs have originally been developed for delivery of other forms of nucleotides such as small interfering RNAs, and usually contain both ionizable cationic lipids and non-charged phospholipids.[15,16] Although a LNP-based mRNA vaccine can also elicit a certain level of Th1 T cell response,[17] it is not known whether such activity is potent enough to mount strong anti-cancer immune responses. So there is a need to explore new platforms for therapeutic mRNA vaccines.

Viruses have been successfully applied to promote cancer immunotherapy,[18,19] and dendritic cells (DCs) sit in the center of anti-tumor immune responses serving as the key linker between innate and adaptive immune responses.[20,21] The body is well equipped to fight against pathogens, and a viral infection will mobilize DCs to the infection site and initiate robust immune responses to destroy the infected cells. Interaction between the pathogen-associated molecular patterns (PAMPs) from the virus and their corresponding pattern-recognition receptors in the DC not only stimulates DC maturation but also promotes secretion of type I interferons (IFN-I) and Th1-biased inflammatory cytokines that prepare the microenvironment for $CD8^+$ T cell stimulation. Many pathogen-derived PAMPs have been identified such as the viral double-stranded RNA, viral single-stranded RNA, and CpG DNA, and have served as important immunostimulants in cancer vaccine development.[22,23]

In this study, we designed a virus-like vaccine particle (VLVP) that resembled a cancer-fighting virus both in structure and in activity. A single-stranded mRNA virus is usually composed of a core that contains negatively charged mRNA molecules and positively charged ribonucleoproteins in a well-defined structure surrounded by a lipid bilayer.[24] To mimic the core structure, we mixed the antigen-encoding mRNA molecules with positively charged protamine. The mRNA-protamine core was then coated with a lipid bilayer formed by both ionizable and non-charged phospholipids. In order to provide potent vaccine activity, we screened a group of toll-like receptor (TLR) ligands and identified one that showed synergy with the particle in stimulating IL-12p70 and TNF-α secretion by DCs. Previous studies by us and others have demonstrated that IL-12p70 and TNF-α levels are essential for DC maturation and for mounting potent anti-tumor immune responses.[25–27] We applied the VLVP to treat a murine tumor model, and demonstrated strong $CD8^+$ T cell activation. In addition, vaccination triggered modification of the tumor microenvironment that favored anti-tumor immune responses. Finally, we delineated underlying mechanism of VLVP-mediated anti-tumor immunity.

2. Results

2.1. VLVP Potently Activates DC Maturation

As the first step to build a VLVP, we mixed eGFP or ovalbumin (OVA)-encoding mRNA molecules with positively charged protamine and then encapsulated the mRNA/protamine core with a lipid shell comprised of cationic lipid EDOPC, helper lipid DOPE, and PEGylated lipid DSPE-PEG2k (Figure S1a, Supporting Information). The core was slightly negatively charged and the final mRNA nanoparticles (mRNA NPs) were positively charged (Figure S1b, Supporting Information). In both cases, encapsulation efficiency was around 80% (Figure S1c, Supporting Information), and the encapsulation process condensed the core (Figure S1d, Supporting Information). Transmission electron microscopy (TEM) revealed a fine core/shell structure of the OVA mRNA NP, and the mRNA/protamine core was more densely stained than the phospholipid bilayer (Figure S1e, Supporting Information). The mRNA molecules could be effectively translated once eGFP mRNA NP was applied to treat DC2.4 dendritic cells, as indicated by fluorescent eGFP protein in the cells (Figure S1f,g, Supporting Information). However, the mRNA NPs could not effectively stimulate DCs based on limited level of changes in DC maturation markers and lack of inflammatory cytokine expression (Figure S1h–j, Supporting Information). The results indicated that an additional PAMP would be needed to activate DC.

PPRs have often served as targets of new vaccine adjuvants, and TLR7 and TLR9 are implicated in viral nucleic acid sensing.[28,29] Among the TLR ligands, unmethylated CpG oligonucleotide (CpG), frequently identified in bacteria and viruses,[30] can potently stimulate TLR9/MyD88 signaling that leads to overexpression of downstream cytokines such as IFN-β and IL-12p70.[31] CL307 and imiquimod are synthetic nucleotide analogs that potently stimulate TLR7 activity.[32] Both CpG and CL307 potently stimulated dose-dependent expression of IL-12p70 and TNF-α in BMDCs, and CpG was more potent than CL307 at the low concentration range. Interestingly, imiquimod did not promote a high level expression of either cytokine (Figure S2, Supporting Information). Based on the result, we prepared VLVP by incorporating CpG into mRNA NP (**Figure 1**a). Gel electrophoresis analysis revealed stable formation of the mRNA/protamine cores when mRNA/CpG was within a 1/0.25 to 1/1 ratio (w/w) (Figure 1b), and size, surface charge and encapsulation efficiency of the resulting VLVPs remained in a close range (Figure 1c–e). TEM analysis revealed well-defined VLVPs with a densely stained core and a lightly stained lipid shell (Figure 1f). We detected a positive correlation between CpG content in the mRNA core and DC maturation based on cell surface CD40, CD80, and CD86 expression levels (Figure 1g–i). In addition, high CpG content significantly raised IL-12p70 and TNF-α expression levels (Figure 1j,k). Based on the results, we concluded that VLVP stimulated DC maturation. VLVPs with a 1:1 CpG-to-mRNA ratio (w/w) were chosen for all further studies.

2.2. VLVP Promotes Antigen Presentation and Cytokine Secretion

We packaged eGFP-encoding mRNA molecules into the optimized VLVP platform and examined particle uptake by DC2.4 cells and BMDCs followed by gene expression and antigen presentation. Fluorescent microscopy detected cells with strong eGFP expression, and flow cytometry revealed comparable rate of expression after cells were treated with mRNA NP or VLVP
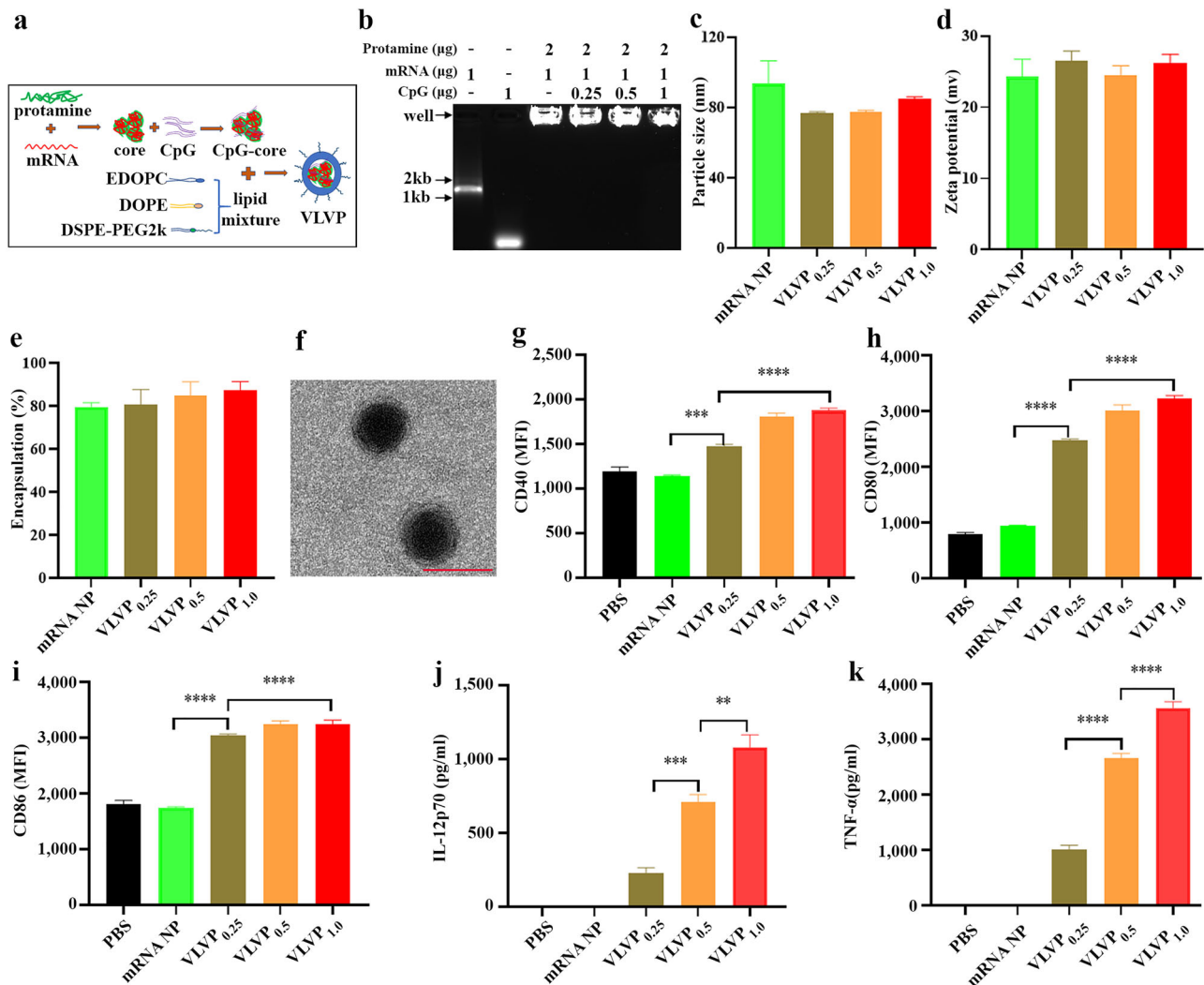
Figure 1. Design, characterization and optimization of VLVP. a) Schematic view of VLVP preparation procedure. b) Agarose gel electrophoresis to show that the mRNA molecules were retained in the loading well once they were packaged in the core. VLVPs containing 0.25, 0.5 and 1 μg CpG are named as VLVP0.25, VLVP0.5, VLVP1.0. c–e) Characterization of mRNA NPs and VLVPs based on particle size, zeta potential, and encapsulation efficiency. Samples were triplicated. f) TEM image of 2 VLVP particles. The mRNA core was densely stained and a thin layer of phospholipid surrounding the core was lightly stained. Scale bar: 100 nm. g–i) Flow cytometry analysis on DC surface markers after BMDCs were treated with mRNA NP or VLVPs for 16 hours. MFI: mean fluorescent intensity. Samples were triplicated. j,k) ELISA assay measurement of IL-12p70 and TNF-α levels in BMDC cell culture after cells were treated with particles for 18 hours. Samples were triplicated. Error bars represent the mean +/– s.e.m.

(**Figure 2**a–c). To determine antigen processing and presentation, we treated BMDCs with OVA-encoding mRNA NP or VLVP. VLVP treatment significantly raised MHC class I molecule (MHCI) expression over mRNA NP, and the contribution was most likely from CpG in VLVP since the mRNA-free vehicle also promoted MHCI expression (Figure 2d). MHCI expression is a relevant parameter since mRNA-derived antigen epitope is presented through the protein.[33] In addition, BMDCs treated with VLVP displayed 20% increase in OVA-MHCI level compared with those treated with mRNA NP (Figure 2e). Interestingly, both CpG and mRNA in VLVP contributed to inflammatory cytokine expression. While mRNA NP treatment did not stimulate IL-6 expression in BMDCs, treatment with mRNA-free vehicle promoted expression of the cytokine and VLVP treatment further raised IL-6 level (Figure 2f). It is well documented that

IL-6 plays an important role in regulating DCs and T cells differentiation.[34,35] A similar trend was observed in expression of IFN-β, a key cytokine in the innate immune sensing pathway,[36] although mRNA NP treatment alone stimulated a low but significant level of cytokine expression over the PBS control (Figure 2g).

Based on these observations, we performed deep RNA sequencing analysis after BMDCs were treated with mRNA NP or VLVP, and systemically analyzed global gene expression. Gene set enrichment analysis detected high expression of genes involved in inflammatory response after treatment with VLVP (Figure 2h), and gene expression heat map showed a group of overexpressed cytokines and chemokines in cells treated with VLVP (Figure 2i). On top of IL-6, IL-12, and TNF-α, the list also included genes encoding additional inflammatory interleukins
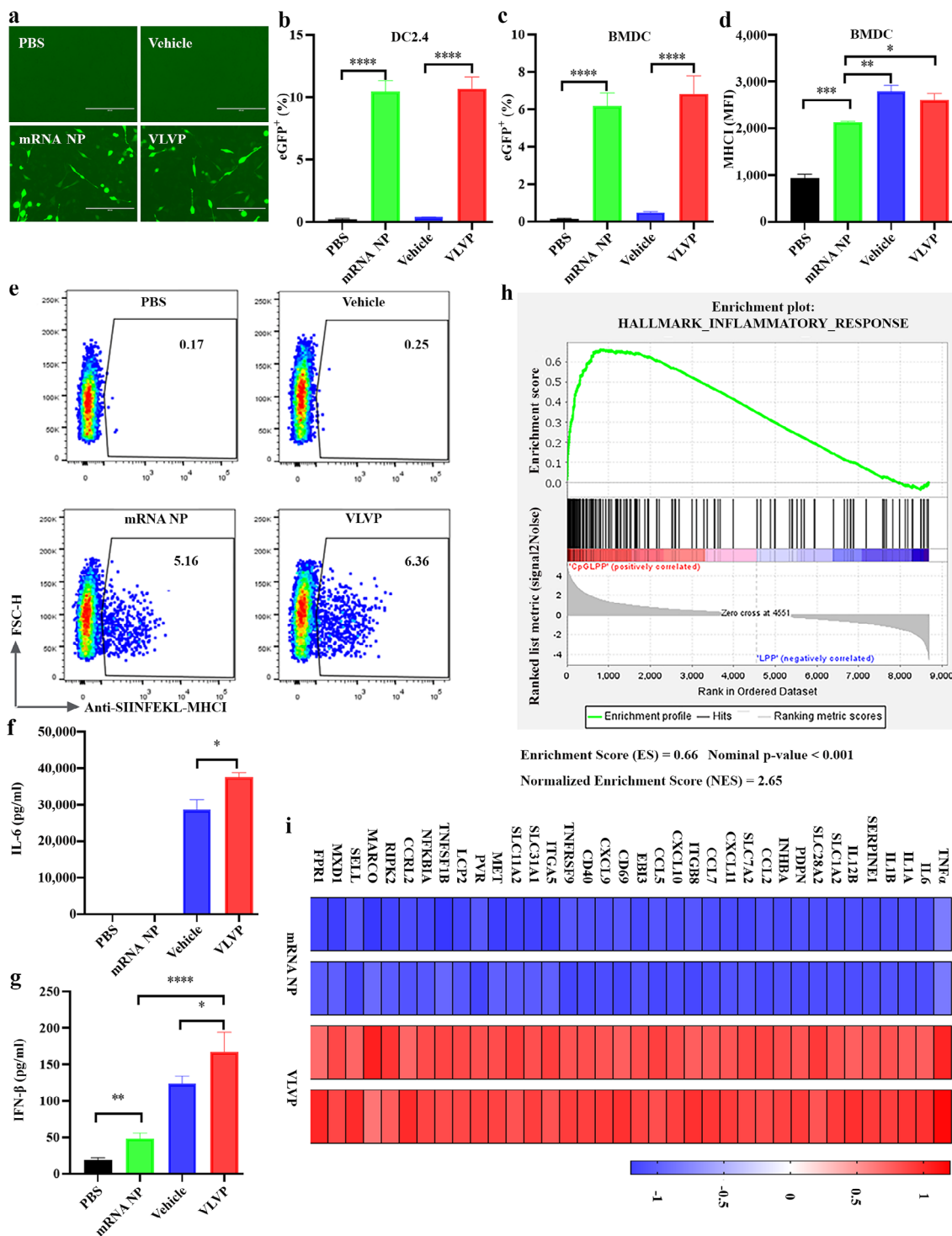
Figure 2. Antigen presentation and cytokine secretion after mRNA NP or VLVP treatment. a) Fluorescent microscopic images of DC2.4 cells treated with mRNA NP or VLVP carrying eGFP-encoding mRNA. Cells with eGFP expression carry dense green fluorescence. Scale bars: 200 μm. b,c) Flow cytometry analysis on eGFP-expressing cells after DC2.4 and BMDC were treated with mRNA NP or VLVP. PBS served as the negative control for mRNA NP, and the mRNA-free vehicle was negative control for VLVP. Samples were triplicated. d) Flow cytometry analysis on MHCI expression after BMDC were treated with OVA-encoding mRNA NP or VLVP. Samples were triplicated. e) Flow cytometry analysis on H-2kb-OVA257–264 presentation in BMDCs after cells were incubated with VLVP or controls for 18 hours. f,g) Cytokine secretion in BMDCs after treatment with VLVP or controls for 18 hours. Samples were triplicated. h) Gene set enrichment analysis (GSEA)-enrichment plot of genes associated with inflammatory response. BMDCs were treated with VLVP or mRNA NP for 16 hours, and cells were collected for RNA sequencing analysis. i) Heat map showing a list of genes encoding inflammatory cytokines/chemokines. Z score was applied to describe the relative gene count. Error bars represent the mean +/− s.e.m. *: $p<0.05$; **: $p<0.01$; ***: $p<0.001$; ****: $p<0.0001$.

**ADVANCED
SCIENCE NEWS**
www.advancedsciencenews.com

**ADVANCED
THERAPEUTICS**
www.advtherap.com

(IL1A and IL1B), C-C motif chemokine ligands (CCL2, CCL7, and the IFN-β-regulated cytokine CCL-5), TNF-related proteins (NFKB1A encoding the NF-κB p105 subunit and TNFRSF9 encoding CD137), and DC and T cell activation markers (CD40 and CD69). It is interesting to note that CD137 is a co-stimulatory immune checkpoint molecule and serves as an activation marker.[37] Our results have clearly indicated that VLVP effectively promoted antigen presentation and inflammatory cytokine secretion.

2.3. VLVP Stimulates T Cell Activation in Lymphatic Organs

mRNA NPs and VLVPs encapsulated with an equal amount of OVA-encoding mRNA were applied to treat mice bearing primary B16OVA tumors, and anti-tumor immune responses were examined. In line with in vitro results, VLVP treatment raised inflammatory cytokine levels in the lymph nodes, while mRNA NP treatment had little effect (**Figure 3**a,b). Surprisingly, both mRNA NP and VLVP could promote T cell activation in the lymph nodes, determined based on the percentage of CD44$^+$ cells, although activated CD8$^+$ T cell level was significantly higher in the VLVP treatment group than the mRNA NP group (Figure 3c). CD44 is a T cell activation marker and is crucial for tumor infiltration of T lymphocytes.[38] ELISpot assay and flow cytometry analysis corroborated with the finding. While both mRNA NP and VLVP raised IFN-γ-secreting cells in the lymph nodes, number of IFN-γ-secreting cells was much higher in the VLVP treatment group (Figure 3d–f). In addition, VLVP treatment, but not mRNA NP treatment, stimulated proliferation of OVA antigen-specific CD8$^+$ T cells (Figure 3g). A similar pattern was observed in splenocytes (Figure 3h–k). Taken together, VLVP activated anti-specific CD8$^+$ T cells to promote anti-tumor immune responses.

2.4. VLVP Facilitates Tumor Infiltration of T Cells and Inhibits Tumor Growth

Anti-tumor activity was also evaluated in mice with primary B16OVA tumors, and significant inhibition of tumor growth was observed in mice vaccinated with VLVP, but not with mRNA NP (**Figure 4**a,b). Flow cytometry analysis of post-treatment tumor samples showed that, while mRNA NP treatment only moderately stimulated IFN-γ^+CD8$^+$ T cells in the tumor, VLVP treatment significantly enriched total CD8$^+$ T cells and dramatically raised IFN-γ^+CD8$^+$ T cell level over both vehicle control and mRNA NP (Figure 4d,e). In line with the finding, we detected a significant higher number of IFN-γ-secreting cells in the post-VLVP treatment tumor samples than other treatment groups based on ELISpot assay (Figure 4e,f). Histological analysis revealed that comparing to the control groups, both mRNA NP and VLVP treatments caused tumor infiltration of CD3$^+$ T lymphocytes, and there were more T cells on the edge of the tumors than inside the tumor bed in both groups (Figure 4g). Quantitative analysis indicated that VLVP was more effective than mRNA NP in facilitating tumor infiltration of T cells (Figure 4h,i). Correlatively, VLVP treatment was more effective in triggering cell death, and consequently leaving less proliferating tumor cells in the tissue (Figure 4g,j,k). The results demonstrate the power of VLVP in mediating anti-tumor immune responses.

2.5. VLVP Treatment Modifies the Tumor Microenvironment

To further evaluate anti-tumor immune responses from the therapeutic agents, we applied time-of-flight mass spectrometer (CyTOF) to systemically analyze subtypes of bone marrow-derived cells in post-treatment tumors. Cells were properly gated, and subpopulations were grouped based on their respective surface markers (Figure S3, Supporting Information). Overall, CD45$^+$ cells accounted for 80–85% all live cells in each sample (Figure S4a, Supporting Information). We observed significant differences on DCs, T cells, and myeloid cells between the VLVP treatment group and the control groups (**Figure 5**a). One obvious difference was the VLVP treatment group had fivefold as many CD8α^+ DCs as in the rest groups (Figure 5b,e). This DC subtype is known for its essential role in cross-presentation and in producing IL-12.[39,40] However, it is also generally accepted that CD8α^+ DCs are tissue residential DCs.[40] The result indicates that VLVP treatment might have promoted proliferation of these cells. In addition, VLVP treatment caused an 80% drop in Arg-1$^+$CD11b$^+$ DC level compared to the vehicle control (Figure S4b, Supporting Information). It has been previously reported that the arginase-1-expressing CD11b$^+$ regulatory DCs could inhibit T cell responses.[41] Eliminating this cell population may provide another route to boost immune responses. Furthermore, VLVP treatment also promoted DC maturation inside the tumor, indicated by increased expression levels of CD80, CD86, and MHCI in CD103$^+$ and CD8$^+$ DCs (Figure S4c, Supporting Information).

Changes in T cells were across the board in the VLVP treatment group (Figure 5c), and magnitude of changes was bigger with CD8$^+$ T cells than CD4$^+$ T cells (Figure 5f,g). There was a fourfold increase in CD8$^+$ T cells comparing to less than 1.5-fold increase in CD4$^+$ T cells in the VLVP treatment group over the PBS control group. In comparison, mRNA NP treatment only brought a minimal level of CD8$^+$ T cell increase, although the change was still statistically significant (Figure 5g). Importantly, number of Ly6C$^+$CD8$^+$ T cells doubled in the VLVP treatment group over the vehicle control group (Figure S4c,d, Supporting Information). A recent study demonstrated this subpopulation of CD8$^+$ T cells had a much higher cancer cell-killing activity than the Ly6C$^-$CD8$^+$ T cells.[42] In addition, VLVP treatment caused dramatic decrease in tumor-associated myeloid cells (Figure 5d,h). It has been well documented that the poorly differentiated myeloid cells produce a large quantity of immunosuppressive cytokines and reactive oxygen species that can dampen anti-tumor immunity.[13,14] Eliminating these cell types is expected to benefit therapeutic efficacy from anti-tumor agents. These results strongly support the notion that VLVP treatment modifies the tumor microenvironment and facilitates anti-tumor immune responses.

2.6. CpG Contributes to Checkpoint Blockade Activity in VLVP

The observation that mRNA NP treatment could significantly raise tumor-infiltrated T lymphocyte (TIL) levels and generate IFN-γ^+CD8$^+$ T cells, although the magnitude was still much lower than in the VLVP treatment group, but did not display any meaningful inhibition of tumor growth was puzzling (Figure 4). To understand the underlying mechanism, we compared
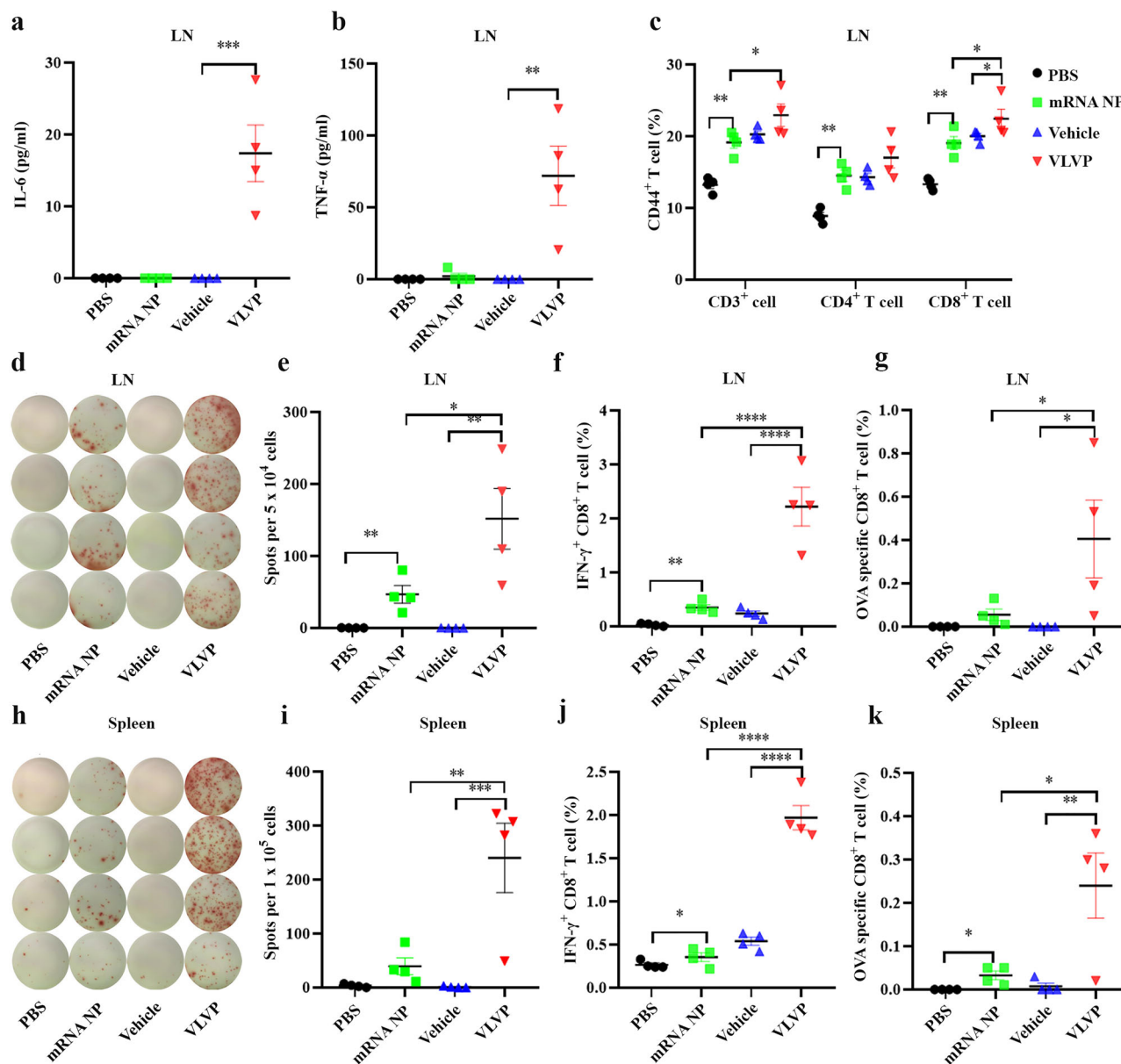
Figure 3. Stimulation of T cell proliferation in lymphatic organs. a,b) IL-6 and TNF-a levels in lymph node (LN) cell suspension after cells were challenged with 10 µg/ml OVA257–264 peptide ex vivo for 24 hours. n=4/group. c) Flow cytometry measurement of CD44$^+$ T cells in LN. n=4/group. d,e) ELISpot measurement on IFN-γ-spot-forming cells after LN cells were challenged ex vivo with SIINFEKL peptide for 24 hours. n=4/group. f) Percentage of IFN-γ^+CD8$^+$ T cells in LN single cells after challenge with 10 µg/ml OVA257–264peptide for 16 hours. n=4/group. g) Percentage of OVA-specific CD8$^+$ T cells in LN single cells. n=4/group. h-i) ELISpot measurement on IFN-γ-spot-forming cells after splenocytes were challenged ex vivo with SIINFEKL peptide for 24 hours. n=4/group. j) Percentage of IFN-γ^+CD8$^+$ T cells in splenocytes after challenge with 10 µg/ml OVA257–264 peptide for 16 hours. n=4/group. k) Percentage of OVAspecific CD8$^+$ T cells in splenocytes. n=4/group. Data are presented as mean +/− s.e.m. *: $p<0.05$; **: $p<0.01$; ***: $p<0.001$; ****: $p<0.0001$.

PD-1 expression levels in TILs from the mRNA NP and VLVP treatment groups. It has been well documented that PD-1 expression contributes to T cell exhaustion and evasion of tumor immunity.[43] We observed dramatic reduction of both PD-1$^+$CD4$^+$ and PD-1$^+$CD8$^+$ T cells in tumors from the VLVP treatment group, but not from the mRNA NP treatment group (**Figure 6**a–c). PD-1$^+$CD8$^+$ T cell levels were also reduced in tumors from the mRNA-free vehicle control group (Figure 6b,c).

The results indicated that inclusion of CpG might have the added benefit of suppressing PD-1 expression in T cells. Interestingly, VLVP treatment raised CTLA4 expression level in Treg cells, but not in CD4$^+$ or CD8$^+$ T cells, although percentage of CTLA4$^+$ Treg cells remained unchanged (Figure S4f,g, Supporting Information). To determine whether PD-1 expression was the major cause of lack of efficacy in the mRNA NP treatment group, we repeated the efficacy study by including anti-PD-1 antibody in the
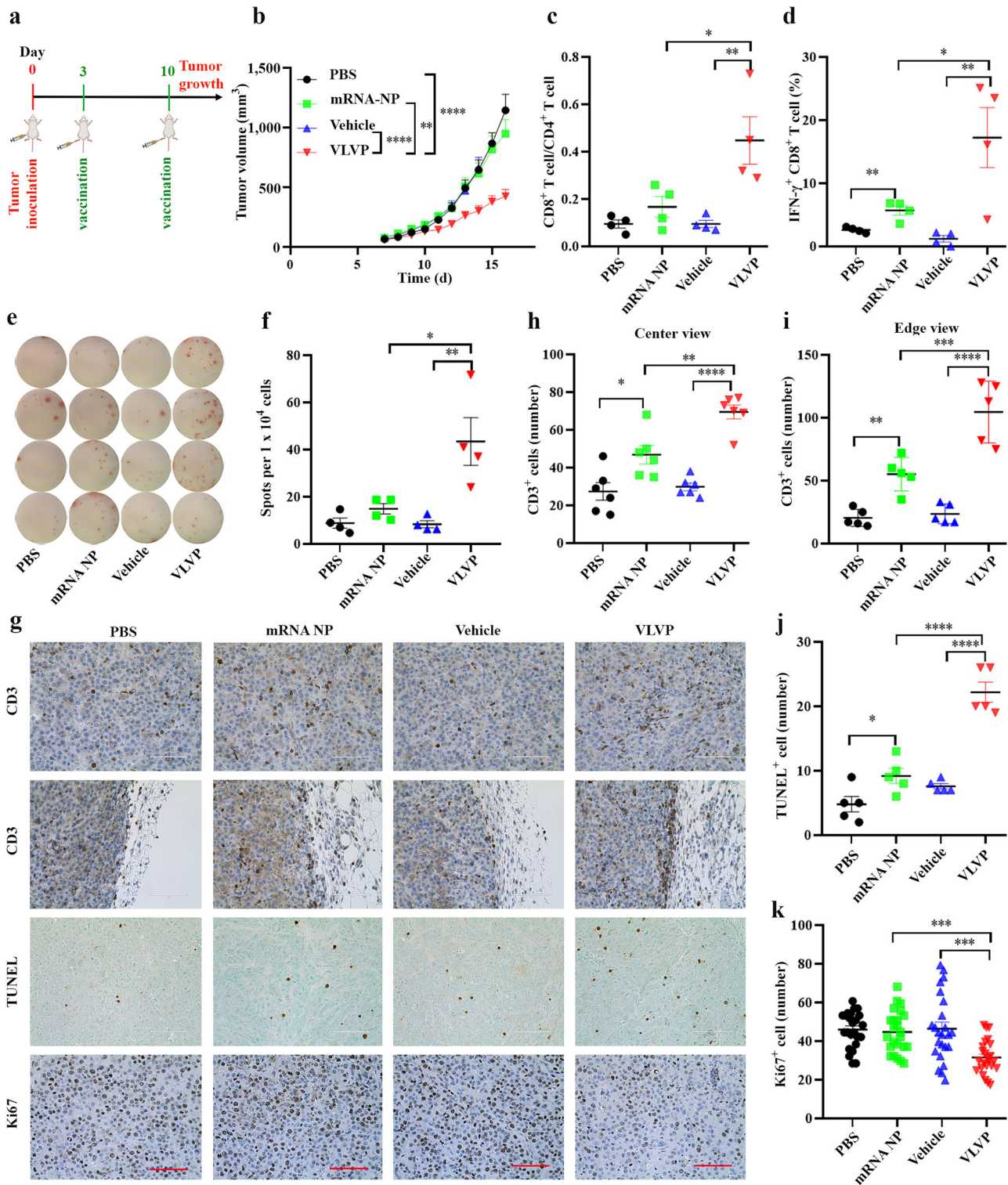
Figure 4. Inhibition of tumor growth by VLVP. a) Schematic view of treatment schedule. b) Tumor growth curves based on daily tumor size change. n = 20 mice/group. c) CD8$^+$ T cell to CD4$^+$T cell ratio in post-treatment tumor tissues based on flow cytometry analysis. d) IFNγ^+ CD8$^+$ T cells in post-treatment tumor tissues based on flow cytometry analysis. e,f) ELISpot analysis on IFN-γ-spot-forming cells in single cell suspensions from post-treatment tumor samples. g) Histological staining of CD3$^+$ T cells, apoptotic cells (by TUNEL), and proliferating cells (by Ki67 staining). h–k) Quantitative analyses of CD3$^+$ T cells, apoptotic cells and proliferating cells based on tissue slides. Data are presented as mean +/– s.e.m. *: $p<0.05$; **: $p<0.01$; ***: $p<0.001$; ****: $p<0.0001$.
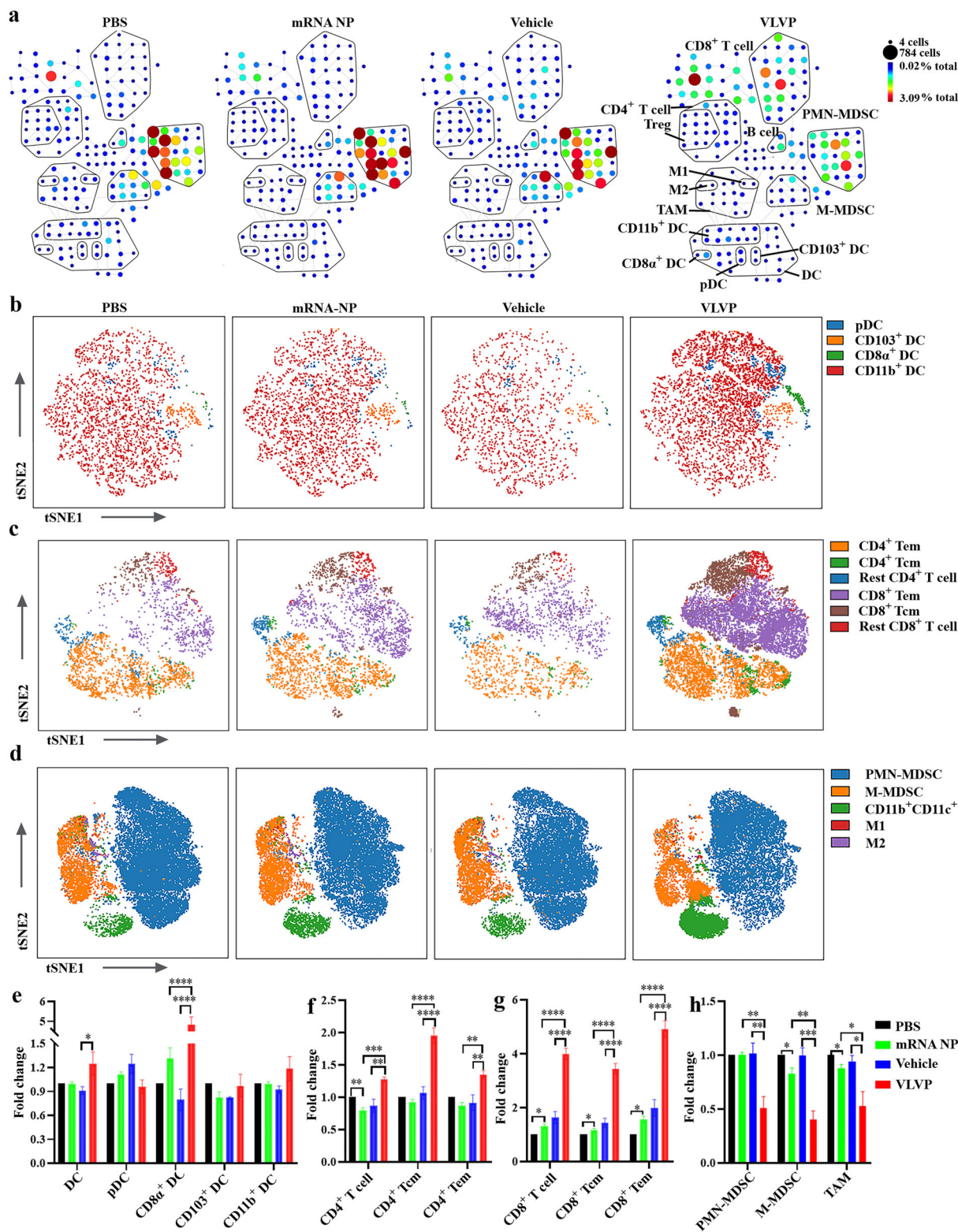
Figure 5. CyTOF analysis of tumor-infiltrated immune cells. C57BL/6 mice (n=3/group) were inoculated with B16OVA cells on day 0, and received treatments on days 3 and 10. Mice were euthanized on day 14 and tumors were harvested for CyTOF analysis. a) Gated CD45$^+$ cells were clustered via spanning-tree progression analysis for density normalized events (SPADE) after staining with 32 markers. The size of a circle represents cell number, and the color represents percentage of cell population in CD45$^+$ cells, as shown at the upper right corner. b) viSNE analysis on CD11c$^+$MHCII$^+$ DCs. c) viSNE analysis on CD45$^+$CD3$^+$ T cells. d) viSNE analysis on CD45$^+$CD11b$^+$ myeloid cells. e–h) Quantitative analyses of DC, T cell, and myeloid cell subpopulations. Data are presented as mean + s.e.m. *: $p<0.05$; **: $p<0.01$; ***: $p<0.001$; ****: $p<0.0001$.
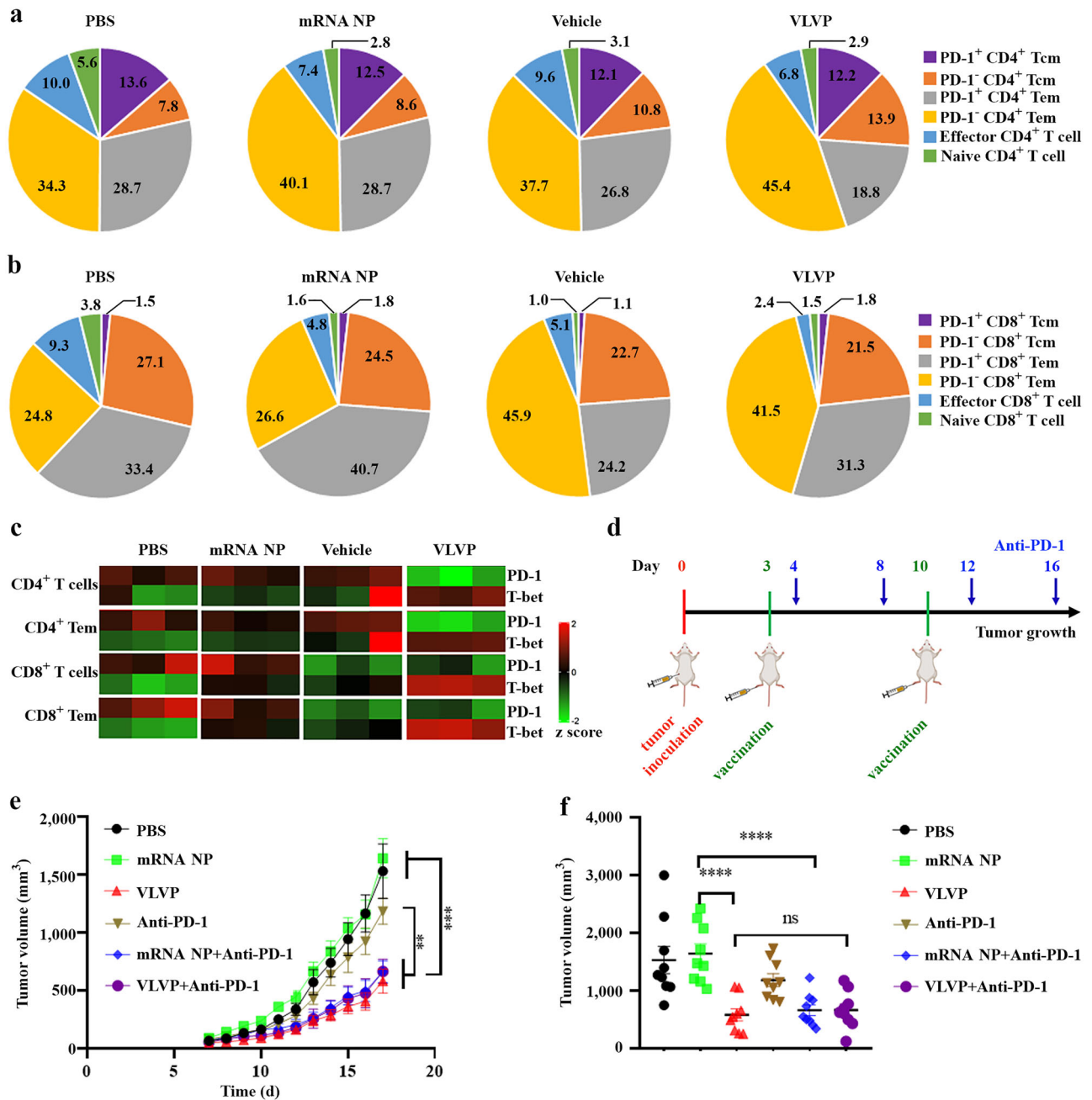
Figure 6. Anti-tumor efficacy from combination therapy with anti-PD-1 antibody. a,b) Subpopulations of CD4$^+$ and CD8$^+$ T cells in post-treatment tumor samples. c) Heatmap showing PD-1 expression in T cell sub-populations from post-treatment tumor samples. d) Schematic view of treatment schedule. e) Tumor growth curves based on daily tumor size change. n = 9 mice/group. f) Plot of tumor volume based on day 17 result. Data are presented as mean + s.e.m. *: $p < 0.05$; **: $p < 0.01$; ***: $p < 0.001$; ****: $p < 0.0001$.

combination groups (Figure 6d). In line with the previous study (Figure 4b), VLVP treatment potently inhibited B16OVA tumor growth, while mRNA NP treatment did not block tumor growth at all (Figure 6d). Interestingly, inclusion of anti-PD-1 antibody did not further improve VLVP efficacy; in contrast, combination of mRNA NP and anti-PD-1 was just as efficacious as the VLVP treatments (Figure 6e,f). The results indicate that CpG in VLVP provided an equivalent benefit of a checkpoint blockade agent.

3. Discussion

In this study, we took a step-by-step approach to build a virus-mimicking mRNA vaccine platform. The resulting VLVP resembles a single-stranded mRNA virus both in structure (with a tight core formed by electrostatic interaction between the negatively charged mRNA and positively charged protein that is surrounded by phospholipid bilayer) and in DC-activating adjuvant activity. It has been well documented that the IFN system plays an

**ADVANCED
SCIENCE NEWS**

www.advancedsciencenews.com

**ADVANCED
THERAPEUTICS**

www.advtherap.com

important role in response to viral infection and that, in the case of a single-stranded mRNA virus, stimulation of the TLR7/MyD88 signaling is a mechanism for overexpression of IFN-I and other inflammatory cytokines.[44] In the current study, we found that the mRNA NPs containing eGFP- or OVA-encoding mRNA molecules could not stimulate cytokine expression or fully promote DC maturation, indicating that an additional component was needed to challenge the body's innate immune system. Incorporation of CpG into the core structure filled the gap and maximized the full potential of a therapeutic cancer vaccine.

We have previously pointed out there exist multiple physical and biological barriers at both systemic level and inside the tumor tissue.[45] Such barriers can block transport of both small molecule drugs and biotherapeutic agents. For an example, treatment with Sipuleucel-T, the first FDA-approved therapeutic cancer vaccine,[46] promoted antigen-specific T cell proliferation; however, most T cells were blocked at the tumor periphery and thus missed the target cells inside the tumor bed.[47] In the current study, we have demonstrated that VLVP is capable of overcoming the physical and biological barriers. Vaccination with VLVP triggered antigen-specific $CD8^+$ T cell proliferation in the lymphatic organs and promoted T cell infiltration deep into the tumor tissue. Several factors may have contributed to the favorable outcome. Secretion of inflammatory cytokines by VLVP-internalized DCs facilitated T cell priming and proliferation. In addition, precipitous drop in immunosuppressive MDSCs and arginase 1-expressing $CD11b^+$ DCs inside tumor further prepared the tissue for T cell infiltration and activity. Furthermore, absence of PD-1 expression maintained T cells at their activation status and enabled effective cancer cell killing.

The observation that treatment with VLVP, but not with the CpG-free mRNA NP, prevented PD-1 overexpression in tumor-infiltrated T cells is intriguing. Although intratumorally injected CpG can lead to T cell activation,[48] it is unlikely that the CpG molecules packaged in VLVP had any direct interaction with the tumor-infiltrated T cells. There is a possibility that VLVP treatment promoted a constant supply of T cells in the lymphatic organs which supported steady tumor infiltration of PD-1^{low} T cells. Alternatively, the tumor microenvironment was depleted with immunosuppressive MDSCs and arginase 1-expressing $CD11b^+$ DCs, and thus prevented T cells from PD-1 overexpression. Regardless of the molecular and cellular mechanism, tumor enrichment of activated T cells in the VLVP-treated mice provided the driving force to mount potent anti-tumor immunity.

Comparing to other non-LNP-based platforms that have been previously described including one from our own laboratory,[49–52] VLVP offers a number of benefits. VLVP can be delivered through intradermal inoculation. The approach prevents leakage of vaccine particles to non-lymphatic organs such as the liver. In addition, both CpG and protamine are FDA-approved drug agents and are biodegradable. Both factors alleviate safety and regulatory concerns. Furthermore, VLVP treatment can also offer the benefit of a checkpoint blockade agent, reducing the burden of a combination therapy with a checkpoint antibody that may also pose a safety concern. Finally, the approach to prepare VLVP is simple and user-friendly.

In conclusion, VLVP offers a potent platform for therapeutic mRNA vaccines. Future efforts will be on translational application of VLVP-based cancer vaccines to benefit patients.

4. Experimental Section

Preparation of Vaccine Particles: mRNA nanoparticles were prepared with phospholipids, protamine, and mRNA. Phospholipids were pre-mixed at a weight ratio of 49: 49: 2 (EDOPC: DOPE: DSPE-PEG2k), and served as the organic phase. Final concentrations were 1.96 mg mL^{-1} EDOPC, 1.96 mg mL^{-1} DOPE, and 0.08 mg mL^{-1} DSPE-PEG2k in the organic phase. Protamine (66.6 µg mL^{-1}) was pre-mixed with mRNA (33.3 µg mL^{-1}) at 1:1 ratio (vol/vol) in a NanoAssemblr (Precision Nanosystems) at a flow rate of 9 mL min^{-1} to form the aqueous phase. The aqueous and organic phases were then mixed together in the NanoAssemblr at a volume ratio of 3:1 to form mRNA NP. Two volumes of phosphate buffer saline (PBS, pH 7.3) were added and the mixture was transferred to an Amicon ultra centrifugal filter (MWCO 30 kDa) followed by centrifugation to remove ethanol. The mixture was washed one more time with 4 volumes of PBS to further remove ethanol during the mRNA concentration process. VLVP particles were prepared by adding CpG into the pre-assembled mRNA-protamine core before the aqueous phase was mixed with the organic phase in the NanoAssemblr.

Animal Studies: All animal procedures were approved by Houston Methodist Research Institute IACUC, AUP-0620-0039. 6–8-week-old C57BL/6 mice were purchased from Charles River Laboratories. All mice were maintained in a pathogen-free facility. Mice were inoculated subcutaneously with B16OVA melanoma cells into the left flank, and vaccinated twice by intra-footpad injection with nanoparticles containing 5 µg mRNA per mouse, once on day 3 and the second time on day 10 after tumor inoculation. Tumor growth was measured on daily basis and tumor volume was calculated as $0.5 \times length \times width^2$. In the combination therapy, anti-PD-1 antibody (200 µg per mouse) was administered intraperitoneally on days 4, 8, 12, and 16.

Statistical Analysis: Two-tailed Student's *t* test was applied for comparison between two groups, and ANOVA with post-hoc test was performed when comparing more than two groups. All statistical analyses were performed using GraphPad Prism8.0.1. Data are presented as means + s.e.m. $P < 0.05$ was considered statistically significant (*: $p < 0.05$; **: $p < 0.01$; ***: $p < 0.001$; ****: $p < 0.0001$).

Supporting Information

Supporting Information is available from the Wiley Online Library or from the author.

Conflict of Interest

The authors declare no conflict of interest.

Author Contributions

H.S. developed the concept and supervised experiments. C.M., Z.C., and S.T. performed cell culture, sample assay, and animal studies. L.H. assisted mRNA particle preparation and Z.Z. offered RNA seq analysis. Q.S.,L.Z., Y.X., J.Z., P.-Y.P., and S.-H.C. provided CyTOF analysis. C.M. and Z.C. performed statistical analysis. C.M., S.-H.C., H.L., and H.S. prepared the manuscript.

Data Availability Statement

The data that supports the findings of this study are available in the supplementary material of this article.

Keywords

adjuvant, cancer, immunotherapy, mRNA vaccine, virus-like vaccine particle

[1] J. A. Wolff, R. W. Malone, P. Williams, W. Chong, G. Acsadi, A. Jani, P. L. Felgner, *Science* **1990**, *247*, 1465.

[2] G. F. Jirikowski, P. P. Sanna, D. Maciejewski-Lenoir, F. E. Bloom, *Science* **1992**, *255*, 996.

[3] N. Pardi, M. J. Hogan, F. W. Porter, *Nat. Rev. Drug Discovery* **2018**, *17*, 261.

[4] J. Nelson, E. W. Sorensen, S. Mintri, A. E. Rabideau, W. Zheng, G. Besin, N. Khatwani, S. V. Su, E. J. Miracco, W. J. Issa, S. Hoge, M. G. Stanton, J. L. Joyal, *Sci. Adv.* **2020**, *6*, eaaz6893.

[5] D. Weissman, K. Kariko, *Mol. Ther.* **2015**, *23*, 1416.

[6] K. S. Corbett, D. K. Edwards, S. R. Leist, O. M. Abiona, S. Boyoglu-Barnum, R. A. Gillespie, S. Himansu, A. Schafer, C. T. Ziwawo, A. T. DiPiazza, K. H. Dinnon, S. M. Elbashir, C. A. Shaw, A. Woods, E. J. Fritch, D. R. Martinez, K. W. Bock, M. Minai, B. M. Nagata, G. B. Hutchinson, C. Wu, C. Henry, K. Bahl, D. Garcia-Dominguez, L. Ma, I. Renzi, W. P. Kong, S. D. Schmidt, L. Wang, Y. Zhang, et al., *Nature* **2020**, *586*, 567.

[7] L. A. Jackson, E. J. Anderson, N. G. Rouphael, P. C. Roberts, M. Makhene, R. N. Coler, M. P. McCullough, J. D. Chappell, M. R. Denison, L. J. Stevens, A. J. Pruijssers, A. McDermott, B. Flach, N. A. Doria-Rose, K. S. Corbett, K. M. Morabito, S. O'Dell, S. D. Schmidt, P. A. Swanson, M. Padilla, J. R. Mascola, K. M. Neuzil, H. Bennett, W. Sun, E. Peters, M. Makowski, J. Albert, K. Cross, W. Buchanan, R. Pikaart-Tautges, et al., *N. Engl. J. Med.* **2020**, *383*, 1920.

[8] K. Servick, *Science* **2020**, *370*, 1388.

[9] U. Sahin, E. Derhovanessian, M. Miller, B. P. Kloke, P. Simon, M. Lower, V. Bukur, A. D. Tadmor, U. Luxemburger, B. Schrors, T. Omokoko, M. Vormehr, C. Albrecht, A. Paruzynski, A. N. Kuhn, J. Buck, S. Heesch, K. H. Schreeb, F. Muller, I. Ortseifer, I. Vogler, E. Godehardt, S. Attig, R. Rae, A. Breitkreuz, C. Tolliver, M. Suchan, G. Martic, A. Hohberger, et al., *Nature* **2017**, *547*, 222.

[10] N. Hilf, S. Kuttruff-Coqui, K. Frenzel, V. Bukur, S. Stevanovic, C. Gouttefangeas, M. Platten, G. Tabatabai, V. Dutoit, S. H. van der Burg, P. Thor Straten, F. Martinez-Ricarte, B. Ponsati, H. Okada, U. Lassen, A. Admon, C. H. Ottensmeier, A. Ulges, S. Kreiter, A. von Deimling, M. Skardelly, D. Migliorini, J. R. Kroep, M. Idorn, J. Rodon, J. Piro, H. S. Poulsen, B. Shraibman, K. McCann, R. Mendrzyk, et al., *Nature* **2019**, *565*, 240.

[11] B. M. Carreno, V. Magrini, M. Becker-Hapak, S. Kaabinejadian, J. Hundal, A. A. Petti, A. Ly, W. R. Lie, W. H. Hildebrand, E. R. Mardis, G. P. Linette, *Science* **2015**, *348*, 803.

[12] P. A. Ott, Z. Hu, D. B. Keskin, S. A. Shukla, J. Sun, D. J. Bozym, W. Zhang, A. Luoma, A. Giobbie-Hurder, L. Peter, C. Chen, O. Olive, T. A. Carter, S. Li, D. J. Lieb, T. Eisenhaure, E. Gjini, J. Stevens, W. J. Lane, I. Javeri, K. Nellaiappan, A. M. Salazar, H. Daley, M. Seaman, E. I. Buchbinder, C. H. Yoon, M. Harden, N. Lennon, S. Gabriel, S. J. Rodig, et al., *Nature* **2017**, *547*, 217.

[13] V. Bronte, S. Brandau, S. H. Chen, M. P. Colombo, A. B. Frey, T. F. Greten, S. Mandruzzato, P. J. Murray, A. Ochoa, S. Ostrand-Rosenberg, P. C. Rodriguez, A. Sica, V. Umansky, R. H. Vonderheide, D. I. Gabrilovich, *Nat. Commun.* **2016**, *7*, 12150.

[14] I. S. Kim, Y. Gao, T. Welte, H. Wang, J. Liu, M. Janghorban, K. Sheng, Y. Niu, A. Goldstein, N. Zhao, I. Bado, H. C. Lo, M. J. Toneff, T. Nguyen, W. Bu, W. Jiang, J. Arnold, F. Gu, J. He, D. Jebakumar, K. Walker, Y. Li, Q. Mo, T. F. Westbrook, C. Zong, A. Rao, A. Sreekumar, J. M. Rosen, X. H. Zhang, *Nat. Cell Biol.* **2019**, *21*, 1113.

[15] G. Basha, T. I. Novobrantseva, N. Rosin, Y. Y. Tam, I. M. Hafez, M. K. Wong, T. Sugo, V. M. Ruda, J. Qin, B. Klebanov, M. Ciufolini, A. Akinc, Y. K. Tam, M. J. Hope, *Mol. Ther.* **2011**, *19*, 2186.

[16] P. R. Cullis, M. J. Hope, *Mol. Ther.* **2017**, *25*, 1467.

[17] U. Sahin, A. Muik, E. Derhovanessian, I. Vogler, L. M. Kranz, M. Vormehr, A. Baum, K. Pascal, J. Quandt, D. Maurus, S. Brachtendorf, V. Lorks, J. Sikorski, R. Hilker, D. Becker, A. K. Eller, J. Grutzner, C. Boesler, C. Rosenbaum, M. C. Kuhnle, U. Luxemburger, A. Kemmer-Bruck, D. Langer, M. Bexon, S. Bolte, K. Kariko, T. Palanche, B. Fischer, A. Schultz, P. Y. Shi, C. Fontes-Garfias, et al., *Nature* **2020**, *586*, 594.

[18] C. J. Breitbach, J. Burke, D. Jonker, J. Stephenson, A. R. Haas, L. Q. Chow, J. Nieva, T. H. Hwang, A. Moon, R. Patt, A. Pelusio, F. Le Boeuf, J. Burns, L. Evgin, N. De Silva, S. Cvancic, T. Robertson, J. E. Je, Y. S. Lee, K. Parato, J. S. Diallo, A. Fenster, M. Daneshmand, J. C. Bell, D. H. Kirn, *Nature* **2011**, *477*, 99.

[19] A. Ribas, R. Dummer, I. Puzanov, A. VanderWalde, R. H. I. Andtbacka, O. Michielin, A. J. Olszanski, J. Malvehy, J. Cebon, E. Fernandez, J. M. Kirkwood, T. F. Gajewski, L. Chen, K. S. Gorski, A. A. Anderson, S. J. Diede, M. E. Lassman, J. Gansert, F. S. Hodi, G. V. Long, *Cell* **2017**, *170*, 1109.

[20] Y. J. Liu, *Cell* **2001**, *106*, 259.

[21] C. Robert-Tissot, D. E. Speiser, *Cancer Discovery* **2016**, *6*, 17.

[22] T. W. Dubensky, Jr., S. G. Reed, *Semin. Immunol.* **2010**, *22*, 155.

[23] R. L. Coffman, A. Sher, R. A. Seder, *Immunity* **2010**, *33*, 492.

[24] H. Yao, Y. Song, Y. Chen, N. Wu, J. Xu, C. Sun, J. Zhang, T. Weng, Z. Zhang, Z. Wu, L. Cheng, D. Shi, X. Lu, J. Lei, M. Crispin, Y. Shi, L. Li, S. Li, *Cell* **2020**, *183*, 730.

[25] X. Xia, J. Mai, R. Xu, J. E. Perez, M. L. Guevara, Q. Shen, C. Mu, H. Y. Tung, D. B. Corry, S. E. Evans, X. Liu, M. Ferrari, Z. Zhang, X. C. Li, R. F. Wang, H. Shen, *Cell Rep.* **2015**, *11*, 957.

[26] B. Pulendran, R. Ahmed, *Nat. Immunol.* **2011**, *12*, 509.

[27] C. Brunner, J. Seiderer, A. Schlamp, M. Bidlingmaier, A. Eigler, W. Haimerl, H. A. Lehr, A. M. Krieg, S. Endres, *J. Immunol.* **2000**, *165*, 6278.

[28] K. Hoshino, T. Kaisho, *Curr. Opin. Immunol.* **2008**, *20*, 408.

[29] M. Gilliet, W. Cao, Y. J. Liu, *Nat. Rev. Immunol.* **2008**, *8*, 594.

[30] A. M. Krieg, A. K. Yi, S. Matson, T. J. Waldschmidt, G. A. Bishop, R. Teasdale, G. A. Koretzky, D. M. Klinman, *Nature* **1995**, *374*, 546.

[31] H. Negishi, Y. Fujita, H. Yanai, S. Sakaguchi, X. Ouyang, M. Shinohara, H. Takayanagi, Y. Ohba, T. Taniguchi, K. Honda, *Proc. Natl. Acad. Sci. USA* **2006**, *103*, 15136.

[32] H. Hemmi, T. Kaisho, O. Takeuchi, S. Sato, H. Sanjo, K. Hoshino, T. Horiuchi, H. Tomizawa, K. Takeda, S. Akira, *Nat. Immunol.* **2002**, *3*, 196.

[33] G. Cafri, A. Sharbi-Yunger, E. Tzehoval, Z. Alteber, T. Gross, E. Vadai, A. Margalit, G. Gross, L. Eisenbach, *Mol. Ther.* **2015**, *23*, 1391.

[34] S. J. Park, T. Nakagawa, H. Kitamura, T. Atsumi, H. Kamon, S. Sawa, D. Kamimura, Y. Ueda, Y. Iwakura, K. Ishihara, M. Murakami, T. Hirano, *J. Immunol.* **2004**, *173*, 3844.

[35] L. Zhou, I. I. Ivanov, R. Spolski, R. Min, K. Shenderov, T. Egawa, D. E. Levy, W. J. Leonard, D. R. Littman, *Nat. Immunol.* **2007**, *8*, 967.

[36] M. B. Fuertes, S. R. Woo, B. Burnett, Y. X. Fu, T. F. Gajewski, *Trends Immunol.* **2013**, *34*, 67.

[37] Z. T. Freeman, T. R. Nirschl, D. H. Hovelson, R. J. Johnston, J. J. Engelhardt, M. J. Selby, C. M. Kochel, R. Y. Lan, J. Zhai, A. Ghasemzadeh, A. Gupta, A. M. Skaist, S. J. Wheelan, H. Jiang, A. T. Pearson, L. A. Snyder, A. J. Korman, S. A. Tomlins, S. Yegnasubramanian, C. G. Drake, *J. Clin. Invest.* **2020**, *130*, 1405.

[38] P. Mrass, I. Kinjyo, L. G. Ng, S. L. Reiner, E. Pure, W. Weninger, *Immunity* **2008**, *29*, 971.

[39] P. Schnorrer, G. M. Behrens, N. S. Wilson, J. L. Pooley, C. M. Smith, D. El-Sukkari, G. Davey, F. Kupresanin, M. Li, E. Maraskovsky, G. T. Belz, F. R. Carbone, K. Shortman, W. R. Heath, J. A. Villadangos, *Proc. Natl. Acad. Sci. USA* **2006**, *103*, 10729.

[40] K. Shortman, W. R. Heath, *Immunol. Rev.* **2010**, *234*, 18.

[41] Q. Y. Liu, C. X. Zhang, A. N. Sun, Y. Y. Zheng, L. Wang, X. T. Cao, *J. Immunol.* **2009**, *182*, 6207.

[42] R. Piranlioglu, E. Lee, M. Ouzounova, R. J. Bollag, A. H. Vinyard, A. S. Arbab, D. Marasco, M. Guzel, J. K. Cowell, M. Thangaraju, A. Chadli, K. A. Hassan, M. S. Wicha, E. Celis, H. Korkaya, *Nat. Commun.* **2019**, *10*, 1430.

[43] L. Chen, X. Han, *J. Clin. Invest.* **2015**, *125*, 3384.

[44] S. S. Diebold, T. Kaisho, H. Hemmi, S. Akira, C. Reis e Sousa, *Science* **2004**, *303*, 1529.

[45] E. Blanco, H. Shen, M. Ferrari, *Nat. Biotechnol.* **2015**, *33*, 941.

[46] P. W. Kantoff, C. S. Higano, N. D. Shore, E. R. Berger, E. J. Small, D. F. Penson, C. H. Redfern, A. C. Ferrari, R. Dreicer, R. B. Sims, Y. Xu, M. W. Frohlich, P. F. Schellhammer, *N. Engl. J. Med.* **2010**, *363*, 411.

[47] L. Fong, P. Carroll, V. Weinberg, S. Chan, J. Lewis, J. Corman, C. L. Amling, R. A. Stephenson, J. Simko, N. A. Sheikh, R. B. Sims, M. W. Frohlich, E. J. Small, *J. Natl. Cancer Inst.* **2014**, *106*, dju268.

[48] S. Wang, J. Campos, M. Gallotta, M. Gong, C. Crain, E. Naik, R. L. Coffman, C. Guiducci, *Proc. Natl. Acad. Sci. USA* **2016**, *113*, E7240.

[49] L. M. Kranz, M. Diken, H. Haas, S. Kreiter, K. Loquai, K. C. Reuter, M. Meng, D. Fritz, F. Vascotto, H. Hefesha, C. Grunwitz, M. Vormehr, Y. Husemann, A. Selmi, A. N. Kuhn, J. Buck, E. Derhovanessian, R. Rae, S. Attig, J. Diekmann, R. A. Jabulowsky, S. Heesch, J. Hassel, P. Langguth, S. Grabbe, C. Huber, O. Tureci, U. Sahin, *Nature* **2016**, *534*, 396.

[50] Y. Wang, L. Zhang, Z. Xu, L. Miao, L. Huang, *Mol. Ther.* **2018**, *26*, 420.

[51] S. Persano, M. L. Guevara, Z. Li, M. Ferrari, P. P. Pompa, H. Shen, *Biomaterials* **2017**, *125*, 81.

[52] M. Fotin-Mleczek, K. M. Duchardt, C. Lorenz, R. Pfeiffer, S. Ojkic-Zrna, J. Probst, K.-J. Kallen, *J. Immunother.* **2011**, *34*, 1.

2100144 (12 of 12)